Regarding the calculation method for a spring-driven gyroscope in rotating aircraft

Nguyen Dinh Duy*, Phan The Son, Do Tien Can, Tran Ngoc Thanh

Institute of Missle, Academy of Military Science and Technology, 17 Hoang Sam, Nghia Do, Hanoi, Vietnam.
*Corresponding author: ariolvietnam@gmail.com
Received 29 Apr. 2025; Revised 2 Jul. 2025; Accepted 20 Sep. 2025; Published 2 Oct. 2025.
DOI: https://doi.org/10.54939/1859-1043.j.mst.106.2025.163-170

ABSTRACT

The study presents a method for calculating spring-driven gyros used in a coordinator for rotating aircraft. By analyzing the relationship between the dimensions of the spiral spring and the gyro rotor, as well as the characteristics of the spiral spring, the authors develop a mathematical model to describe the motion of the spring-driven gyro during its spin-up and operational phases. Additionally, a method for determining the key kinematic parameters of this gyroscope type is proposed. The simulation results showed that the spring-driven gyroscope has a short start-up time of 0.017 s, a maximum rotational speed of 21,000 rpm, a drift around the outer frame axis not exceeding 5° within 20 s, and a frame-folding time of 60 s. These characteristics meet the requirements for gyroscopes used in rotating aircraft with short operating duration.

Keywords: Rotating aircraft; Gyro coordinator; Spring-driven gyroscope; Spiral spring.

1. INTRODUCTION

To control a aircraft rotating around its longitudinal axis, the control signal must be converted from the ground control station's coordinate system to the aircraft-mounted coordinate system. This task is solved by the gyro-type command distributor, also known as the gyro-coordinator. In certain types of rotating aircraft, a critical requirement for gyroscopes is their ability to achieve rapid start-up, typically within 0.1–0.2 seconds [1, 2]. The gyro rotor in these objects can be spun up by many different methods, such as using a pull cord, propellant, compressed air, or springs. The first inventions of spring-driven gyroscopes were announced in the early 1950s of the 20th century [3, 4]. In comparison to gyros starting up by pull cords, compressed air and pyro gyros [1, 2, 5, 6], spring-driven gyroscopes have numerous advantages: high overload resistance, elimination of bearing jamming from combustion byproducts, compact size, reduced mass, and advanced technological integration.

Spiral springs, leaf springs and elastic parts are widely used in a number of devices as energy storage sources to move other mechanisms [7-10]. Previously published documents mainly focus on calculating the basic characteristics of spiral springs in tightly wound and deflated states, as well as methods of manufacturing, checking and testing them within measuring devices. Specific calculations for spring-driven gyroscopes have not been widely published. The results of the study [11] showed the possibility of a fast starting up of the spring-driven gyroscope, however, a detailed calculation of the characteristics of the gyroscope is not mentioned. Therefore, the study of calculation methods for spring-driven gyroscopes is both theoretically and practically significant, supporting research and development of new-generation rotating aircraft and contributing to advancements in technological autonomy.

2. PROBLEM

2.1. Relationship between spiral spring and rotor size

Suppose: r_1 – Inner radius of the spring after being deflated; r_2 – Outer radius of the spring tightly wound on the shaft; n_1 – Number of turns of the spring after being deflated; n_2 – Number of turns of the tightly wound spring; n – Number of turns of the rotor; r_0 – Radius of the wound

shaft; R_0 – Inner radius of the rotor (figure 1); h – Thickness of spring, then we have:

$$n_1 = \left(R_0 - r_1\right)/h;\ n_2 = \left(r_2 - r_0\right)/h \tag{1}$$

In this case, it is assumed that the end sections AB and CD of the spring, which are not adjacent to the shaft during or to the rotor during unwinding, are small compared to the working length of the spring [8].

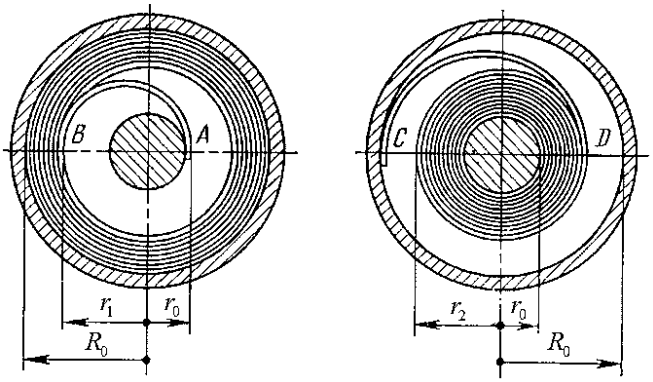

***Figure 1**. Spiral spring placed in a rotor [10].*

Each revolution of the rotor, when the spring is released, reduces the number of spring windings on the shaft by one turn. Therefore, the number of revolutions of the rotor after the spring is fully unwound is:

$$n = n_2 - n_1 = \left(r_1 + r_2 - R_0 - r_0\right)/h \tag{2}$$

Since the surface area of the spring in the deflated and tightly wound states is equal, we have:

$$\pi\left(R_0^2 - r_1^2\right) = \pi\left(r_2^2 - r_0^2\right),$$

Therefore,

$$r_2 = \sqrt{R_0^2 + r_0^2 - r_1^2} \tag{3}$$

Substituting equation (3) into equation (2), we obtain:

$$n = \left(r_1 + \sqrt{R_0^2 + r_0^2 - r_1^2} - R_0 - r_0\right)\Big/h \tag{4}$$

Equation (4) shows that the number of revolutions of the rotor is a function of the variable r_1. To find the maximum value of this function, we calculate its derivative, set it equal to zero, and solve the resulting equation, which yields:

$$r_1 = r_2 = \sqrt{\left(R_0^2 + r_0^2\right)/2} \tag{5}$$

Equation (5) shows that the rotor reaches its maximum number of revolutions when it contains a spring whose length satisfies the condition r_1=r_2. The spring that enables the rotor to achieve the maximum number of revolutions upon being deflated is called the “standard” spring.

A “standard” motor is defined as a spring motor characterized by an optimal ratio between the length of the spiral spring and the dimensions of the rotor and winding shaft, ensuring that the rotor achieves the maximum number of revolutions. In a standard motor, the volume of the spring in the tightly wound state and in the deflated state is equal; that is, the outer radius of the spring remains the same in both states.

Based on the equality of the spring volume in the tightly wound and deflated states, we can calculate the length of the spring.

$$L = \pi\left(R_0^2 - r_0^2\right)/(2h) \tag{6}$$

Since the "standard" motor, with the minimum rotor size, ensures the greatest number of revolutions, it is therefore used in spring-driven gyroscopes.

2.2. Torque generated by spiral spring

Figure 2 [6, 7] shows the characteristics of a free spiral spring (solid line) and the spring winding and unwinding diagram, considering Hysteresis (dashed line).

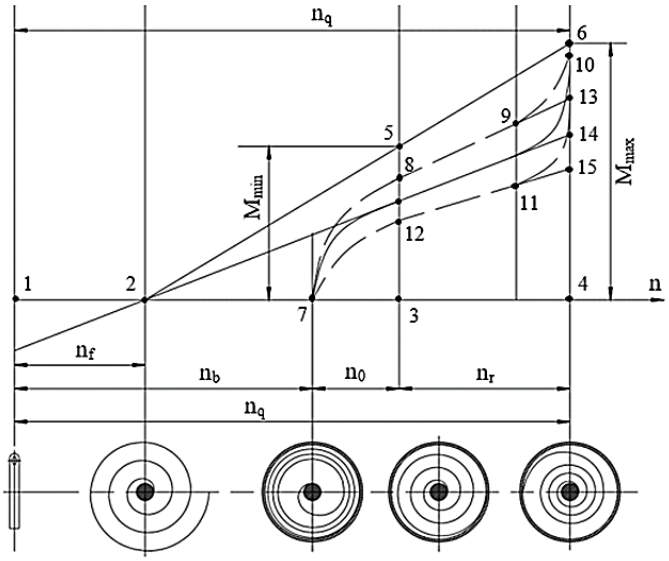

***Figure 2**. Working diagram of a spiral spring placed inside the rotor.*

In figure 2: n_f – Number of turns of the spiral spring in free state; n_b – Number of turns of the spiral spring in unwound state; n_q – Number of turns of the spiral spring in tightly wound state; n_r – Number of working turns of the spiral spring.

Applying the equation for the change in angle between two adjacent cross-sections of a thin bar [8, 9], we obtain the following:

$$d\varphi = MdS/EJ = PydS/EJ \tag{7}$$

in which: E – Young modulus, $J = bh^3/12$ – Moment of inertia of the spring cross section, dS – Unit length element of the spring.

By integrating equation (7), we obtain the formula for calculating the rotation angle of the final cross-section of the spiral spring when it is wound on the shaft:

$$\varphi = \int_0^L \frac{MdS}{EJ} = \frac{ML}{EJ}$$

The torque produced by the spiral spring can be expressed as:

$$M = EJ\varphi/L = Ebh^3\pi n/(6L) \tag{8}$$

The maximum and minimum values that the spiral spring can produce in the free state (solid line in figure 2) are as follows:

$$M_{\max} = Ebh^3\pi\left(n_q - n_f\right)/(6L);\ M_{\min} = Ebh^3\pi\left(n_q - n_f - n_r\right)/(6L)$$

Due to friction between the windings, when the spring, placed in the rotor, is deflated, its

maximum and minimum moments will be smaller than in the ideal case and are calculated as follows:

$$\begin{cases} M^b_{\min} = \dfrac{K\left(M_{\max} + M_{\min}\right)}{1+\nu}; M^b_{\max} = \nu M^b_{\min} \\ \nu = \dfrac{\left(1+K\right)\nu_M + K - 1}{1 + K - \left(1-K\right)\nu_M}; \nu_M = \dfrac{M_{\max}}{M_{\min}} \end{cases}$$

where, K is the quality factor. Its value mainly depends on the type of attachment of its outer end to the inner wall of the rotor and is determined experimentally [6, 7].

2.3. Calculation of the spring-driven gyro using the standard motor

Kinematic equation of the starting process of the gyro rotor [5]:

$$\left(J_r + J_{sp}\left(t\right)\right)\frac{d\Omega}{dt} + \Omega\frac{dJ_{sp}\left(t\right)}{dt} = M^b_{\max} - A_1 n \tag{9}$$

in which, $n = \dfrac{1}{2\pi}\int_0^t \Omega dt$; $A_1 = \dfrac{M^b_{\max} - M^b_{\min}}{n_r}$; J_r – Moment of inertia of the rotor; J_{sp} – Instantaneous moment of inertia of the spring pressing against the rotor wall during spring descent; n – Number of revolutions of the winding shaft or rotor during spring descent.

The above mathematical model is an approximate model because it is based on certain simplifications, and in equation (9), the resistance moment is not considered. Additionally, this equation does not account for the effect of centrifugal force on the moment characteristics of the spring.

When the rotor spins up, the rotor rotates while the shaft remains stationary. The mass of the spring, once released, will be added to the mass of the rotor. Since the starting time is typically very short, it can be assumed that the moment of inertia of the rotor increases linearly.

$$J\left(t\right) = J_r + \beta t;\ \beta = J^b_{sp}/t \tag{10}$$

in which, Jr – Rotor moment of inertia; J^b_{sp} – Moment of inertia of the fully deflated spring, pressed against the rotor wall, t – Rotor spin-up time. Substituting equation (10) into equation (9), we obtain:

$$\left(J_r + \beta t\right)\frac{d\Omega}{dt} + \beta\Omega = M^b_{\max} - \frac{A_1}{2\pi}\int_0^t dt \tag{11}$$

Integrating equation (11) in closed form is impossible, however, if we assume that:

$$J\left(t\right) = J_r + J^b_{sp}/2 = J_1 = const \tag{12}$$

then, the solution of equation (11) can be found. With Assumption (12), equation (11) can be rewritten in the following form:

$$J_1\frac{d\Omega}{dt} + \beta\Omega = M^b_{\max} - \frac{A_1}{2\pi}\int_0^t dt \tag{13}$$

Using the Laplace transform with zero initial conditions (i.e., t = 0, Ω = 0), we can express equation (13) in operator form and find the rotor rotation speed:

$$\Omega(s) = \frac{F_1(s)}{F_2\left(s\right)} = \frac{2\pi s M^b_{\max}}{2\pi J_1 s^2 + 2\pi s\beta + A_1} \tag{14}$$

The equation $F_2(s)=0$ has two distinct solutions:

$$s_{1,2} = -\frac{\beta}{2J_1} \pm \sqrt{\frac{\beta^2}{4J_1^2} - \frac{A_1}{2\pi J_1}} \approx -\frac{\beta}{2J_1} \pm i\sqrt{\frac{A_1}{2\pi J_1}}$$

therefore, the original function Ω(t) can be found by the following formula:

$$\Omega(s) = \frac{M_{\max}^{b}}{\sqrt{\frac{A_1 J_1}{2\pi}}} e^{\frac{-\beta t}{2J_1}} \sin\left(\sqrt{\frac{A_1}{2\pi J_1}} t\right) \tag{15}$$

After starting, the gyro rotor operates by inertia, gradually decreasing its rotational speed. The run-up process of the gyro rotor is expressed by the following equation:

$$J_1 \, d\Omega / dt = -\left(M_{ms} + M_a\right) \tag{16}$$

in which, M_{ms} – Friction torque, M_a – Aerodynamic drag torque, which is calculated according to formula [12]:

$$M_a(t) = 1{,}1 \cdot 10^{-7} \rho^{0,7} \mu^{0,3} \Omega^{1,7}(t) \oint_{Lr} r^{3,4} dl$$

in which: ρ – Density of air; μ - Air kinematic viscosity coefficient; Ω - Rotor rotation speed; *r* - Rotor radius.

3. RESULTS AND DISCUSSION

Figure 3 shows a model of a spring-driven rotor mounted in a Cardan frame.

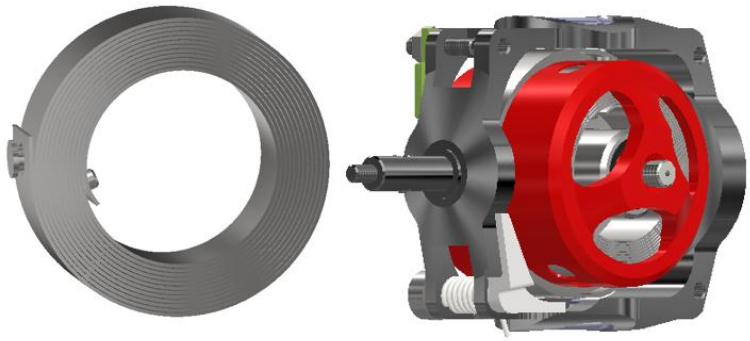

Figure 3. *Spiral spring (a) and gyro rotor model (b) in the gyro-coordinator 9Б861.*

The characteristics of the gyro-coordinator 9Б861 are shown in table 1 [5]:

Table 1. *Characteristics of the gyro-coordinator 9Б861.*

Parameter	**Value**
Maximum rotor speed, rpm	20 000
Rotor speed reduction in 20 seconds, %	20
Frame folding time, not less than, s	40
Acceleration time, s	0,02

Based on equations (15) and (16), the process of starting up and running up of a spring-driven gyroscope, the spring of which is made of 3J21 alloy (GB/T 14992 China), has been simulated. Parameters of the gyromotor are shown in table 2.

Figure 4a shows the dependence of the rotor rotation speed on the thickness of the spiral spring with a width of 8 mm. When the spring thickness increases from 0.1 mm to 0.32 mm, the rotor speed increases and reaches a maximum value of 21,000 rpm. As the thickness increases further,

the speed decreases. These values are consistent with the published parameters of the spring-driven gyro in the gyro-coordinator 9Б861 [5].

Figure 4b shows that after 20 seconds, the rotor rotation speed decreases by no more than 20%, meeting the technical requirements for gyro-coordinator [5].

Table 2. *Parameters of the gyromotor.*

Parameter	**Value**
Shaft radius, mm	4.8
Rotor radius, mm	13
Rotor moment of inertia, kg·m^2	10^{-6}
Young's modulus of 3J21 alloy, MPa	$2{,}1 \cdot 10^5$
Spring length, mm	594
Spring thickness, mm	0.32
Spring width, mm	8
Spring moment of inertia, kg·m^2	$1.21 \cdot 10^{-6}$
Number of turns in a tightly wound state	13.5
Number of turns in deflated state	9
Number of working turns	3.3
Friction torque around the rotor's axis of rotation, N·m	$3 \cdot 10^{-4}$
Maximum aerodynamic drag torque around the rotor's axis of rotation, N·m	$1.5 \cdot 10^{-11}$
Maximum kinetic moment of the rotor, N·m·s	$4 \cdot 10^{-3}$
Disturbing moments around the outer frame axis, N·m [13]	$8.8 \cdot 10^{-5}$
Disturbing moments around the inner frame axis, N·m [13]	$1.8 \cdot 10^{-5}$

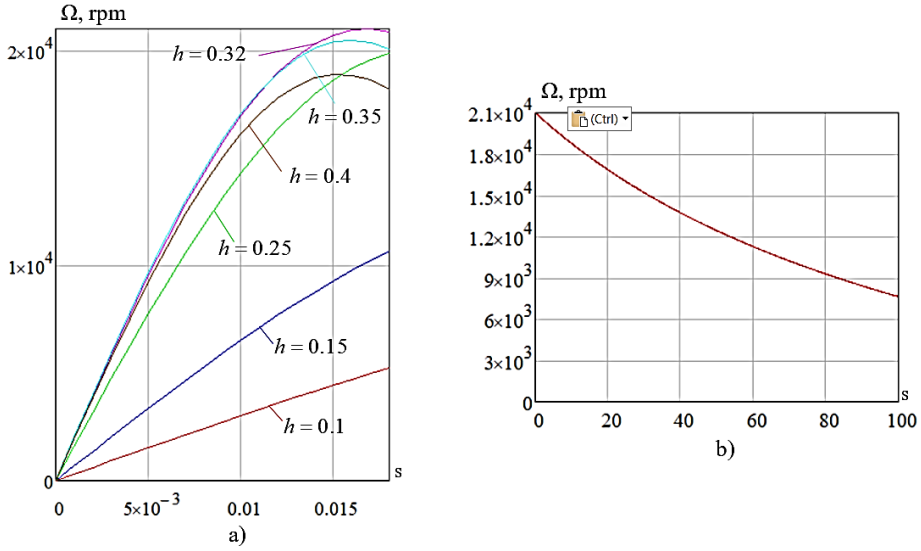

Figure 4. *Speed of the gyromotor during starting-up (a) and running-up (b).*

Taking into account the values of the disturbing moments around the axes of the outer and inner frames, the gyroscope drift around the outer frame axis does not exceed 5 degrees in 20 seconds, and the frame-folding time is at least 60 seconds, as shown in figure 5.

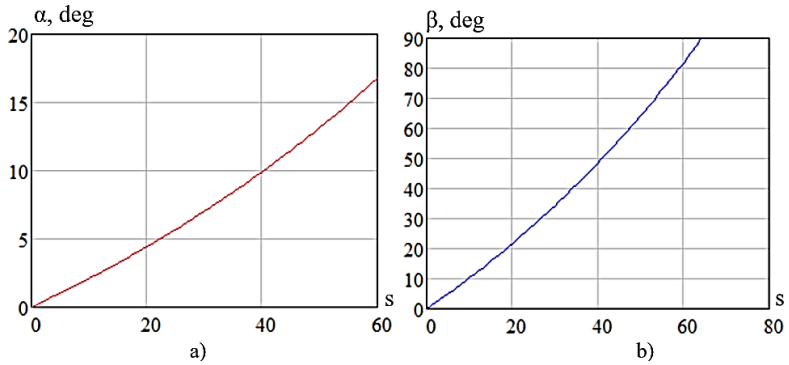

Figure 5. *Gyroscope drifts around the axis of the outer (a) and inner (b) frame.*

4. CONCLUSIONS

Based on the results obtained, the following conclusions can be drawn:

– Based on the calculation of the spiral spring, equation (15) determines the dependence of gyro rotor speed on the parameters of the gyro rotor and spring.

– The numerical simulation results show that the gyroscope, with rotor and spring parameters as shown in table 2, accelerates to a maximum speed of 21,000 rpm with a spring thickness of 0.32 mm. The start-up time of the rotor is 0.017 seconds. These results closely match the published data from spring-driven gyroscope manufacturers for the gyro-coordinator 9Б861.

– The gyroscope drift around the axis of the outer frame does not exceed 5 degrees in 20 seconds, and the frame-folding time is at least 60 seconds, which meets the requirements for the gyroscope used on rotating aircraft.

The research results can be used as a reference for preliminary design calculations of rotating aircraft with short operating duration.

REFERENCES

[1]. Бабичев, В. И. *"Разработка бортовых гироскопов противотанковых управляемых артиллерийских снарядов"*/ В. И. Бабичев, М. В. Грязев // Известия Тульского государственного университета. Технические науки. № 9-2, С. 9-19, (2017).

[2]. Распопов, В. Я. *"Становление и развитие гироскопии в Туле"*/ В. Я. Распопов // Известия Тульского государственного университета. Технические науки. № 1,. С. 3-28, (2021).

[3]. Patent US2732721. Spring-driven gyroscopes, (1956).

[4]. Patent US3434354. Spring-driven gyroscopes, (1969).

[5]. Горин В. И., Распопов В. Я. *"Гирокоординаторы вращающихся по крену ракет"*. Москва : НТЦ "Информтехника", (1996).

[6]. Распопов В. Я. *"Гироприборы и системы управляемых ракет ближней тактической зоны"*. М-во образования и науки РФ, ФГБОУ ВПО, Тул. гос. ун-т,. - Тула : Изд-во ТулГУ - 247 с, (2013).

[7]. Андреев Г.Н., Марков Б.Н., Педь Е.И. *"Теория механизмов и детали точных приборов"*. Учеб. пособие для машиностроит. Техникумов. М. : Машиностроение, 269 с, (1987).

[8]. Гевондян Т. А. *"Пружинные двигатели. Теория, расчет, методы контроля и испытаний"*. Москва : Гос. изд-во оборонной промышленности – 366 с, (1956).

[9]. Андреева Л. Е. *"Упругие элементы приборов"*/ под редакцией д-ра техн. наук, проф. В. И. Феодосьева. - Москва : Машгиз - 454 с, (1962).

[10]. Пономарев С. Д., Андреева Л. Е. *"Расчет упругих элементов машин и приборов"*. Изд. Машиностроение, (1980).

[11]. Jiang Renfu, Ding Zhixin. *"A Study on the Starting up Time for a Spring Driven Gyroscope"* [J]. Transactions of Beijing institute of Technology, (6): 680-684, (1996).

[12]. Бабаева Н.Ф. и др. *"Расчёт и проектирование элементов гироскопических устройств"*. М.: Машиностроение. 480 с, (1967).

[13]. Nguyen Phu Thang, Nguyen Dinh Duy. *"Xây dựng chương trình mô phỏng phương trình chuyển động của con quay tên lửa chống tăng B-72".* Journal of Military Science and Technology. Special Issue, Institute of Missle, (2016).

TÓM TẮT

Về một phương pháp tính toán con quay lò xo trên khí cụ bay quay quanh trục dọc

Bài báo trình bày phương pháp tính toán con quay lò xo sử dụng trong bộ tọa độ trên khí cụ bay quay quanh trục dọc. Trên cơ sở phân tích mối liên hệ giữa kích thước lò xo xoắn ốc và rô to con quay, cũng như các đặc tính của lò xo xoắn ốc, các tác giả xây dựng mô hình toán mô tả chuyển động con quay lò xo khi khởi động và chạy đà, đồng thời đưa ra phương pháp tính toán các thông số động học chính của kiểu con quay này. Kết quả mô phỏng cho thấy, con quay lò xo có thời gian khởi động ngắn (0,017 s), vận tốc tối đa đạt 21000 vòng/phút, độ trôi của khung ngoài trong 20 s không vượt quá 5º, thời gian chập khung là 60 s, đáp ứng được các yêu cầu đối với con quay sử dụng trên khí cụ bay quay quanh trục dọc với thời gian làm việc ngắn.

Từ khoá: Khí cụ bay; Bộ tọa độ con quay; Con quay lò xo; Lò xo xoắn ốc.